

**Theoretical insights into the electroreduction of nitrate to ammonia on the
graphene-based single-atom catalyst**

Yuanyuan Wang,^{1,4} Donghai Wu,^{1,2,4} Peng Lv,^{1,4} Bingling He,^{1,4} Xue Li,^{1,4},
Dongwei Ma,^{1,4*} and Yu Jia^{1,3,4*}

¹*Key Laboratory for Special Functional Materials of Ministry of Education, and School of
Materials Science and Engineering, Henan University, Kaifeng 475004, China*

²*Henan Key Laboratory of Nanocomposites and Applications, Institute of Nanostructured
Functional Materials, Huanghe Science and Technology College, Zhengzhou 450006, China*

³*International Laboratory for Quantum Functional Materials of Henan, and School
of Physics, Zhengzhou University, Zhengzhou 450001, China*

⁴*Joint Center for Theoretical Physics, and Center for Topological Functional Materials,
Henan University, Kaifeng 475004, China*

Supporting Information

*Corresponding author. E-mail: madw@henu.edu.cn; (D. Ma).

*Corresponding author. E-mail: jiayu@henu.edu.cn (Y. Jia).

Table S1 Zero-point energy corrections (ΔE_{ZPE}) and entropic contributions ($T\Delta S$) (at 298.15 K) to the free energies of the key intermediates.

Species	ΔE_{ZPE} (eV)	$T\Delta S$ (eV)
NO_3^*	0.42	0.23
NO_3H^*	0.61	0.33
NO_2^*	0.27	0.20
HNO_2^*	0.55	0.20
NO_2H^*	0.55	0.20
HNO_2H^*	0.84	0.34
NO^* -end	0.19	0.09
NO^* -side	0.16	0.14
HNO^* -end	0.47	0.18
HNO^* -side	0.46	0.15
HNOH^*	0.78	0.17
NH^*	0.32	0.12
NH_2^*	0.68	0.10
$\text{NO}_2^*+\text{OH}^*$	0.64	0.29
NO^*+OH^*	0.54	0.25
HNO^*+OH^*	0.85	0.23
$\text{H}_2\text{NO}^*+\text{OH}^*$	1.17	0.30
O^*+OH^*	0.44	0.15
H_2NO^*	0.78	0.20
H_2NOH^*	1.13	0.22
$\text{H}_2\text{N}^*+\text{OH}^*$	1.05	0.18
O^*	0.06	0.11
OH^*	0.34	0.13

Table S2 Zero-point energy corrections (ΔE_{ZPE}) and entropic contributions ($T\Delta S$) (at 298.15 K) to the free energies of the relevant molecules, and their free energy correction ($\Delta G_{\text{correct}}$) referenced to the experimental formation energy.

Species	ΔE_{ZPE} (eV)	$T\Delta S$ (eV)	$\Delta G_{\text{correct}}$ (eV)
HNO ₃ (g)	0.70	0.83	1.06
HNO ₂ trans(g)	0.53	0.77	0.67
NO ₂ (g)	0.23	0.74	0.93
NH ₃ (g)	0.89	0.60	0.18
H ₂ (g)	0.27	0.40	--
H ₂ O(g)	0.56	0.67	--

Table S3 The key parameters of the TMN₃@G and TMN₄@G systems. Average distance ($d_{\text{TM-N}}$) between the embedded TM atom and its bonded N atoms, binding energy (E_b) of the TM atom with respect to the N-doped graphene and the isolated metal atom, net charge (ΔQ) of the TM atom, spin magnetic moment (M) of the whole system (the value outside the parenthesis) and the embedded TM atom (the value inside the parenthesis).

TMN _x	$d_{\text{TM-N}}$ (Å)	E_b (eV)	ΔQ (e)	M (μ_B)
TiN ₃	1.95	-5.22	-1.74	2.19 (1.58)
VN ₃	1.95	-7.05	-1.50	2.44 (2.64)
CrN ₃	1.96	-3.86	-1.26	4.56 (3.87)
MnN ₃	2.01	-4.10	-1.15	5.32 (4.89)
FeN ₃	1.87	-4.92	-1.16	3.26 (3.29)
CoN ₃	1.83	-5.21	-0.92	2.30 (2.11)
NiN ₃	1.84	-4.60	-0.93	1.47 (1.26)
TiN ₄	2.04	-8.24	-1.88	1.46 (1.32)
VN ₄	1.98	-7.82	-1.68	2.78 (2.60)
CrN ₄	1.95	-6.89	-1.55	3.99 (3.68)
MnN ₄	1.92	-6.79	-1.60	3.02 (3.20)
FeN ₄	1.90	-7.62	-1.32	2.00 (2.03)
CoN ₄	1.88	-7.92	-1.01	0.98 (0.82)
NiN ₄	1.88	-7.76	-1.01	0.00 (0.00)

Table S4 Binding free energy of NO_3^- ($\Delta G(\text{NO}_3^*)$) and H ($\Delta G(\text{H}^*)$), the net charge of the NO_3^* , and the distance between the O atoms in NO_3^* and its bonded TM atom.

TMN _x	$\Delta G(\text{NO}_3^*)$ (eV)	$\Delta G(\text{H}^*)$ (eV)	$\Delta Q(\text{NO}_3^*)$ (e)	$d(\text{M-O}^*)$ (Å)
TiN ₃	-3.62	-0.65	0.86	2.12, 2.14
VN ₃	-3.23	-0.45	0.82	2.06, 2.13
CrN ₃	-3.44	-0.34	0.83	2.02, 2.04
MnN ₃	-2.71	-0.31	0.78	2.01, 2.01
FeN ₃	-2.66	0.42	0.76	1.99, 1.99
CoN ₃	-2.45	0.01	0.70	1.95, 1.95
NiN ₃	-2.11	0.23	0.67	1.93, 1.93
TiN ₄	-3.37	-0.49	0.78	2.13, 2.14
VN ₄	-2.73	-0.12	0.82	2.06, 2.06
CrN ₄	-1.33	0.32	0.75	1.93
MnN ₄	-0.87	0.48	0.79	2.03
FeN ₄	-0.70	0.32	0.68	1.91
CoN ₄	-0.55	0.12	0.66	1.94
NiN ₄	0.20	1.61	0.68	2.21

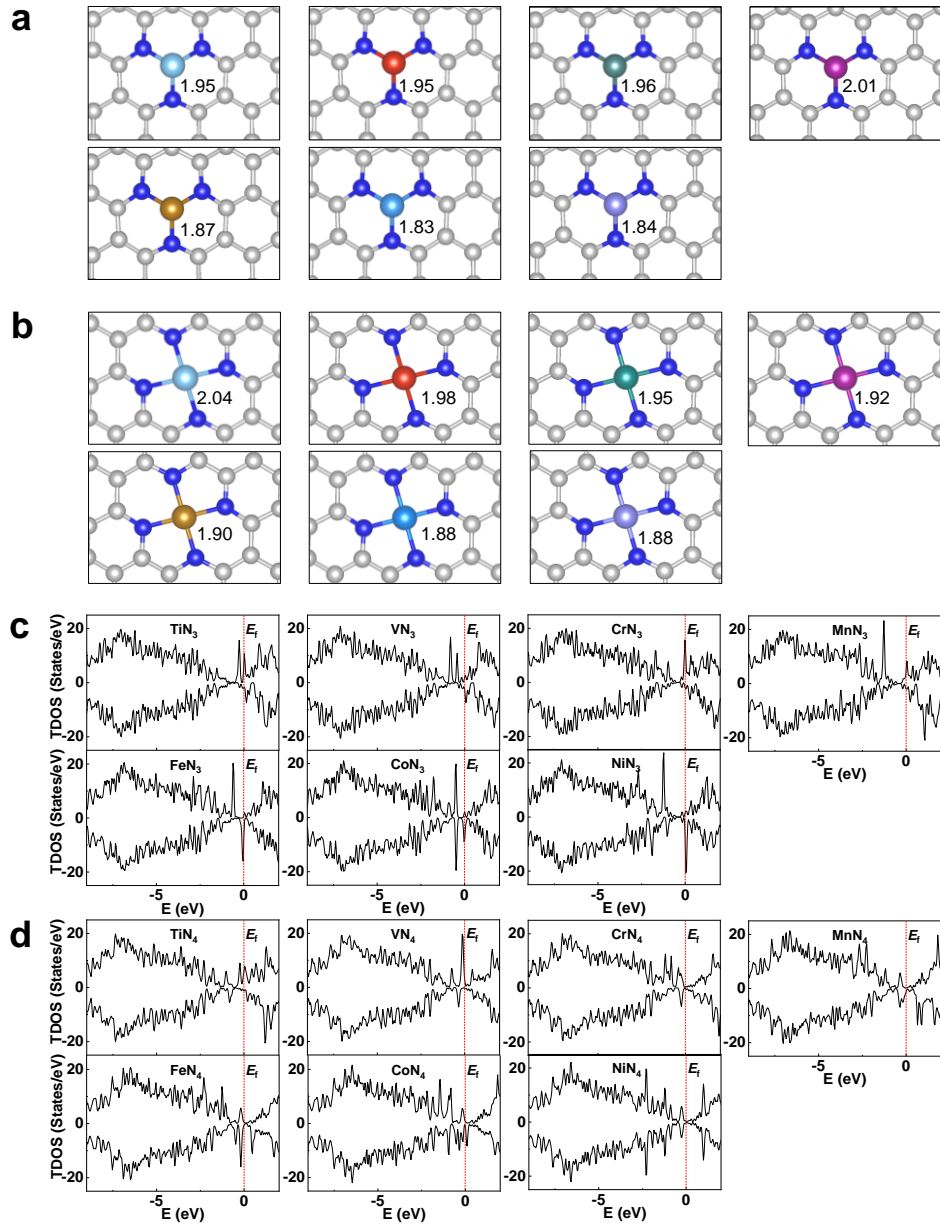


Fig. S1. The atom configurations with TM-N bond lengths (in Å) of the TMN₃@G (a) and TMN₄@G (b) systems. The total densities of states (TDOS) of the TMN₃@G (c) and TMN₄@G (d) systems. The vertical dashed line denotes the position of Fermi level (E_f). The positive and negative values of TDOS correspond to the spin-up and spin-down states, respectively.

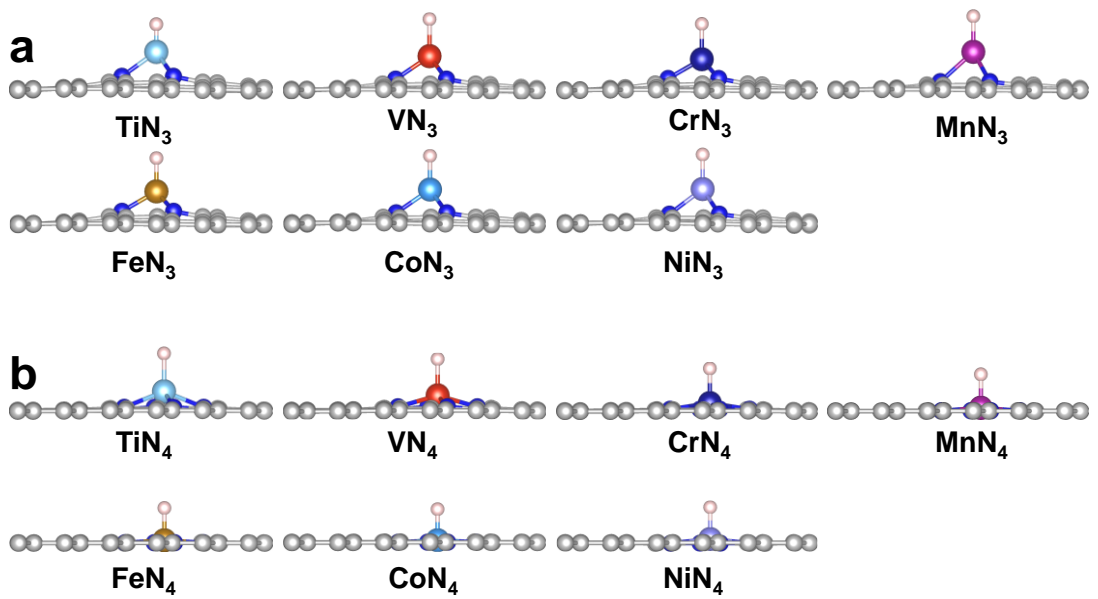


Fig. S2. The most stable adsorption configurations of H atoms on TMN₃@G (a) and TMN₄@G (b).

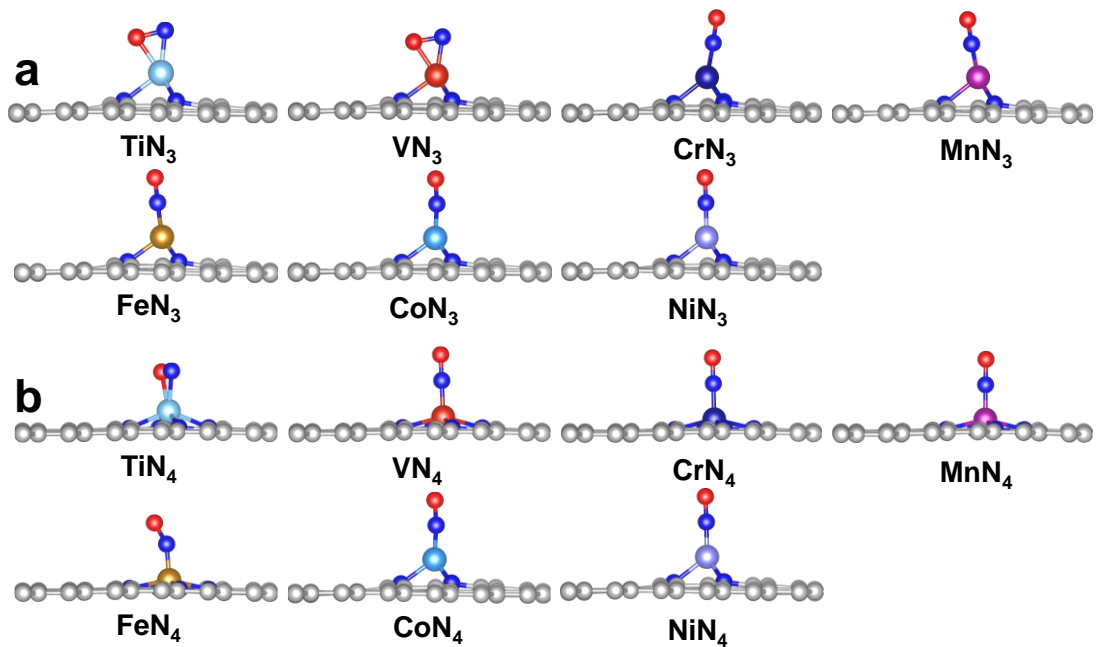


Fig. S3. The most stable adsorption configurations of NO molecules on TMN₃@G (a) and TMN₄@G (b).

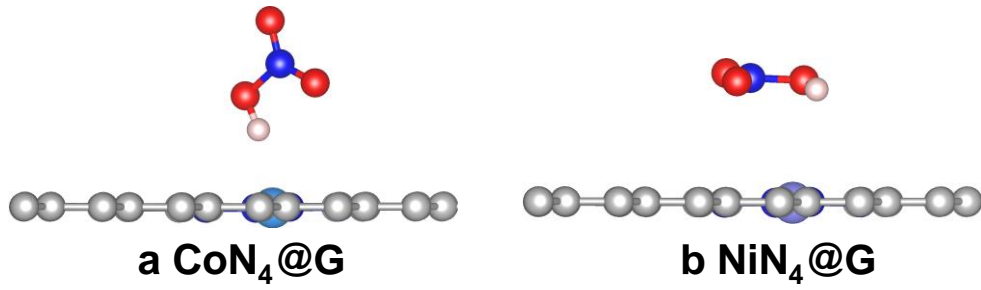


Fig. S4. The most stable configurations of HNO_3^* for $\text{CoN}_4@\text{G}$ (a) and $\text{NiN}_4@\text{G}$ (b).

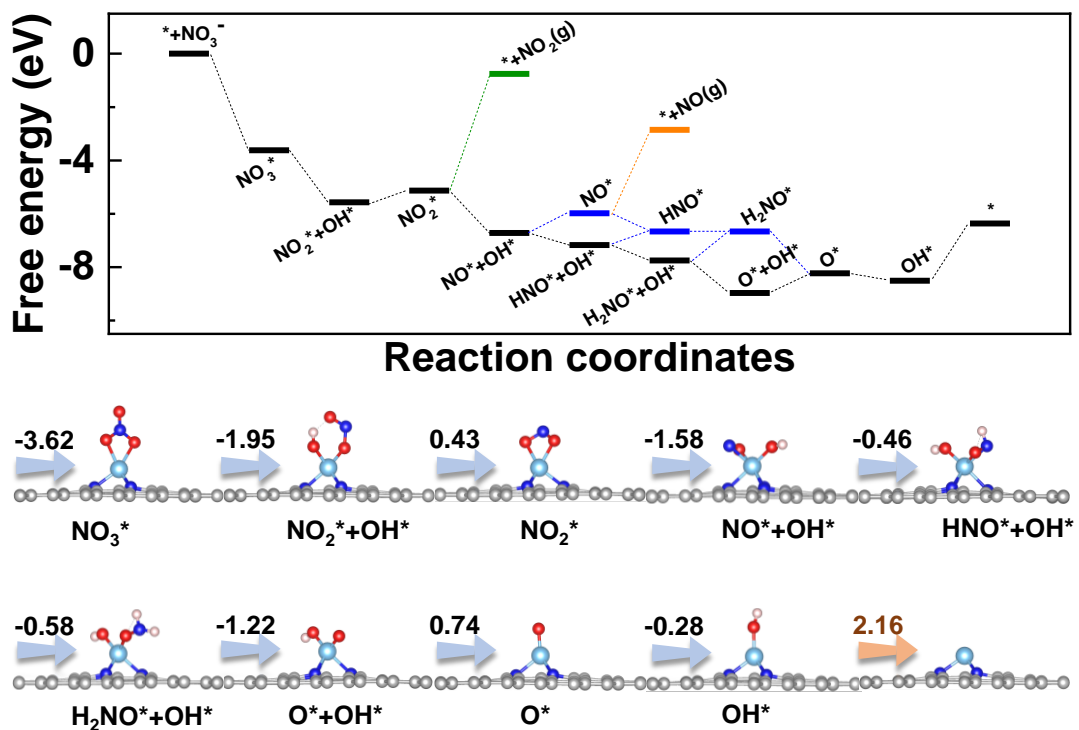


Fig. S5. Free energy diagram together with the configurations of corresponding intermediates for the e NO_3 RR on $\text{TiN}_3@\text{G}$.

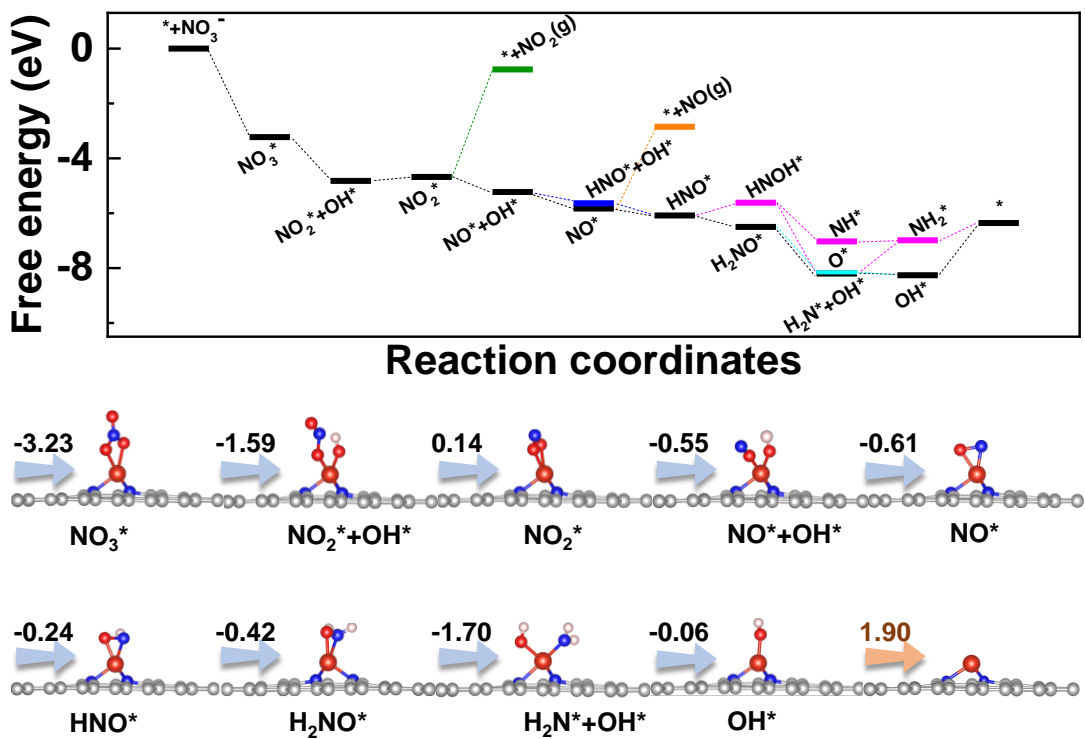


Fig. S6. Free energy diagram together with the configurations of corresponding intermediates for the e NO_3 RR on $\text{VN}_3@\text{G}$.

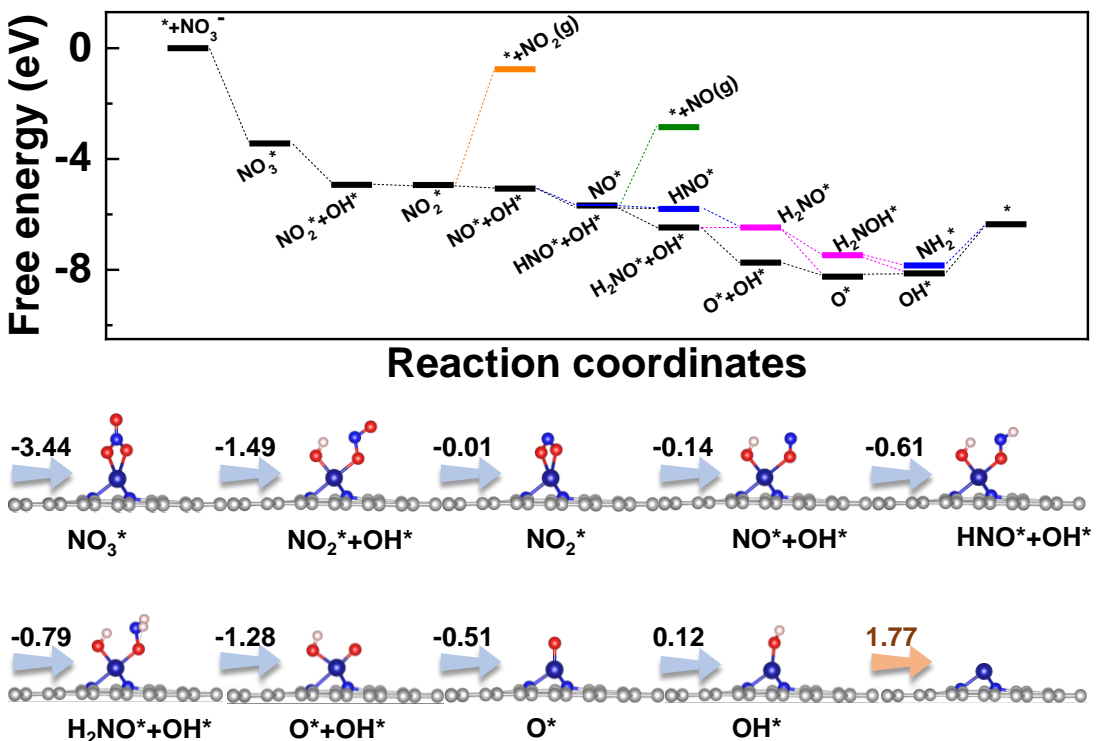


Fig. S7. Free energy diagram together with the configurations of corresponding intermediates for the e NO_3 RR on $\text{CrN}_3@\text{G}$.

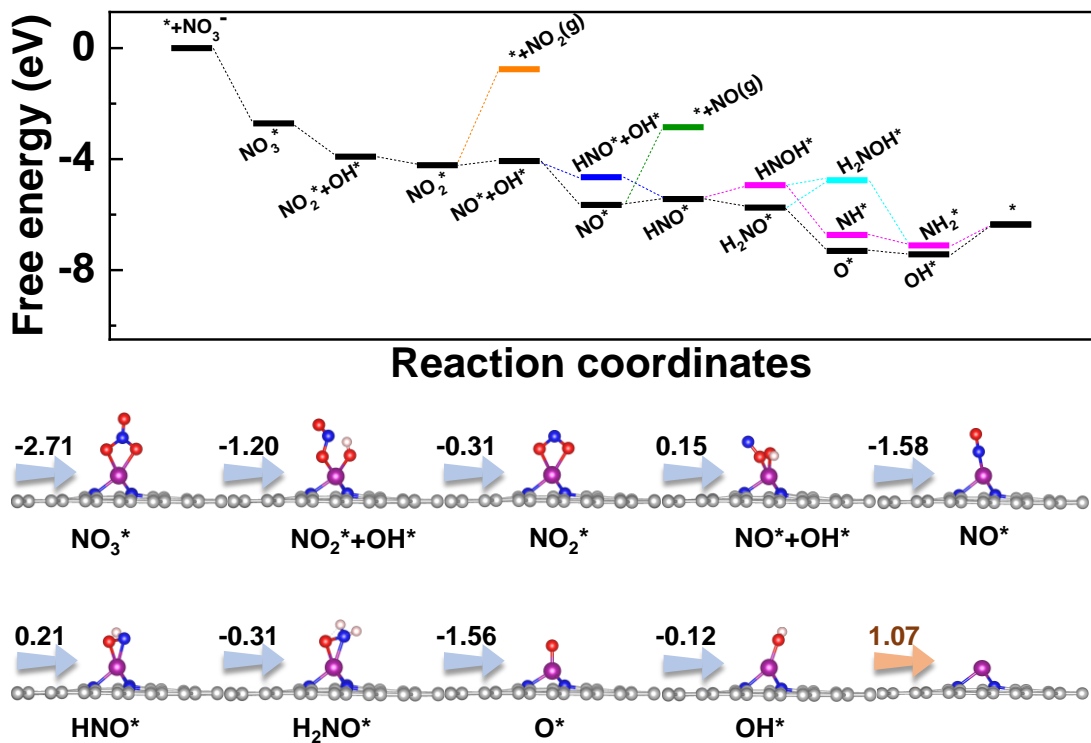


Fig. S8. Free energy diagram together with the configurations of corresponding intermediates for the e NO_3 RR on $\text{MnN}_3@\text{G}$.

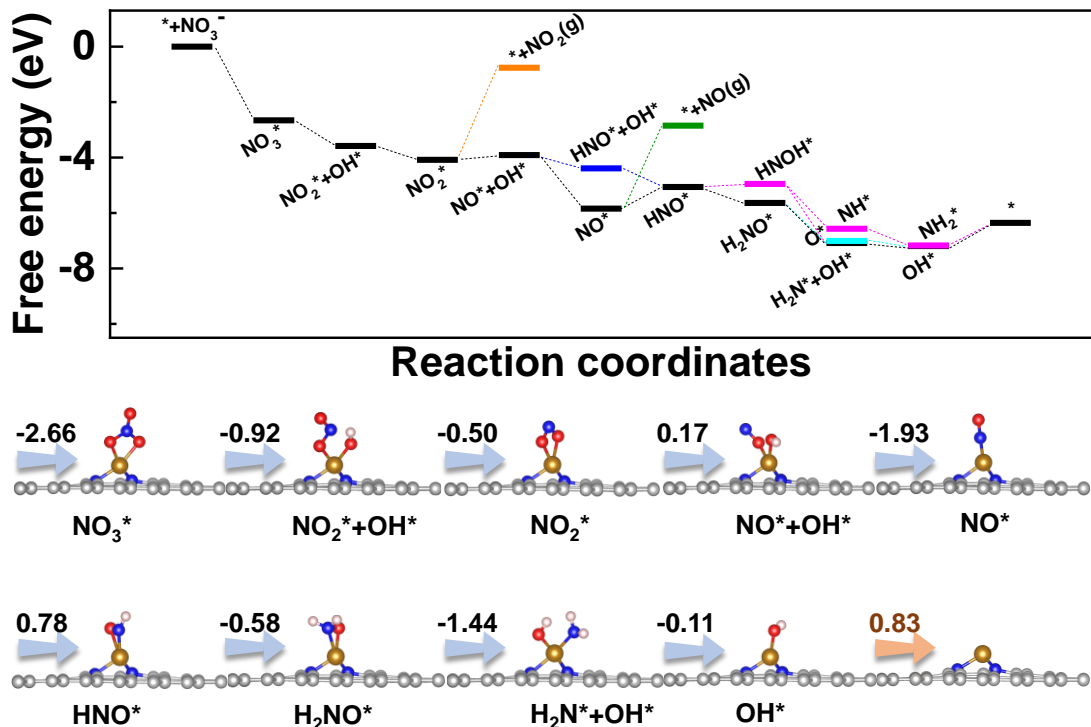


Fig. S9. Free energy diagram together with the configurations of corresponding intermediates for the e NO_3 RR on $\text{FeN}_3@\text{G}$.

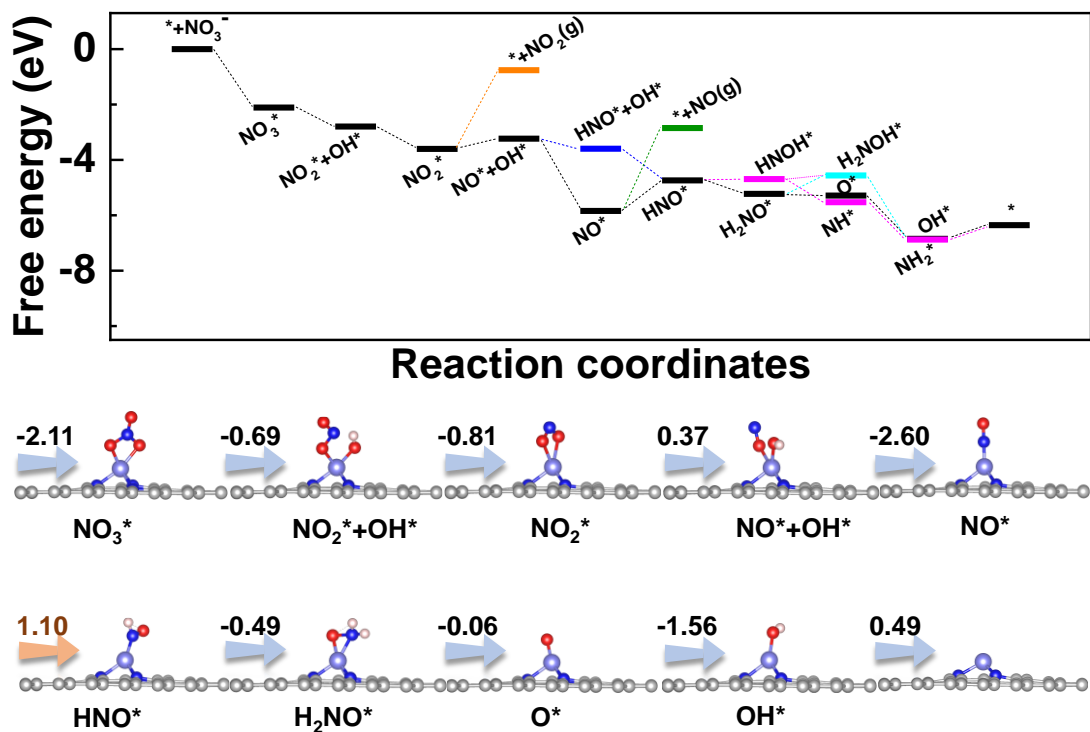


Fig. S10. Free energy diagram together with the configurations of corresponding intermediates for the e NO_3 RR on $\text{NiN}_3@\text{G}$.

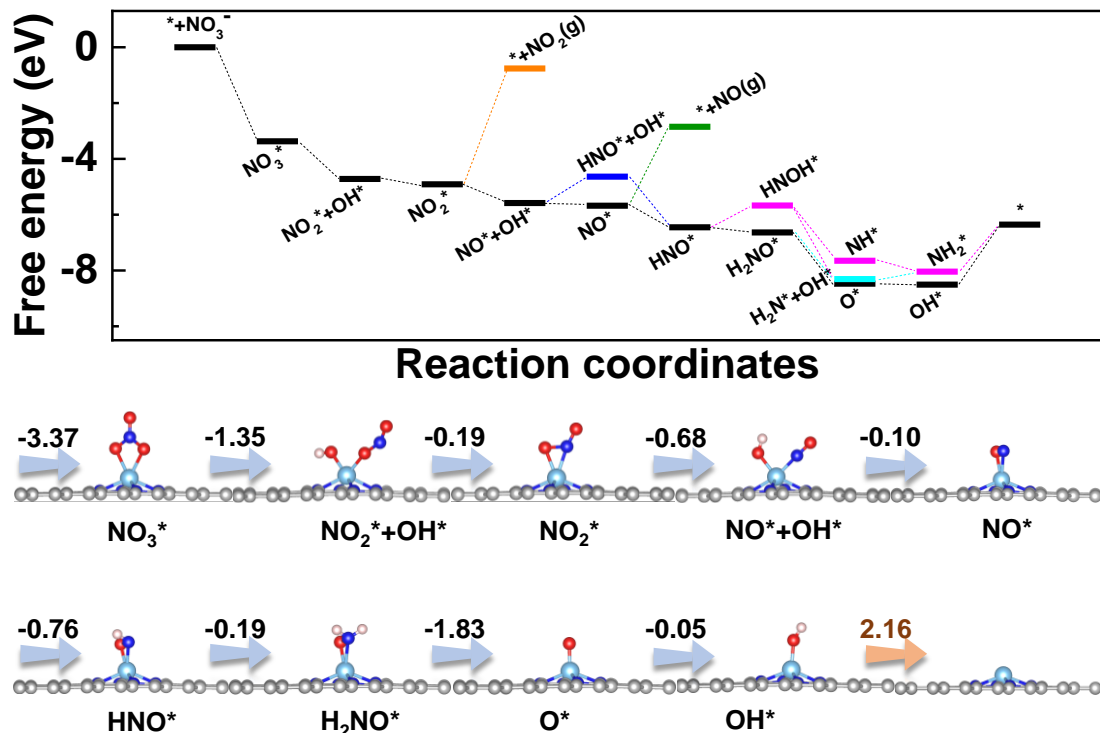


Fig. S11. Free energy diagram together with the configurations of corresponding intermediates for the e NO_3 RR on $\text{TiN}_4@\text{G}$.

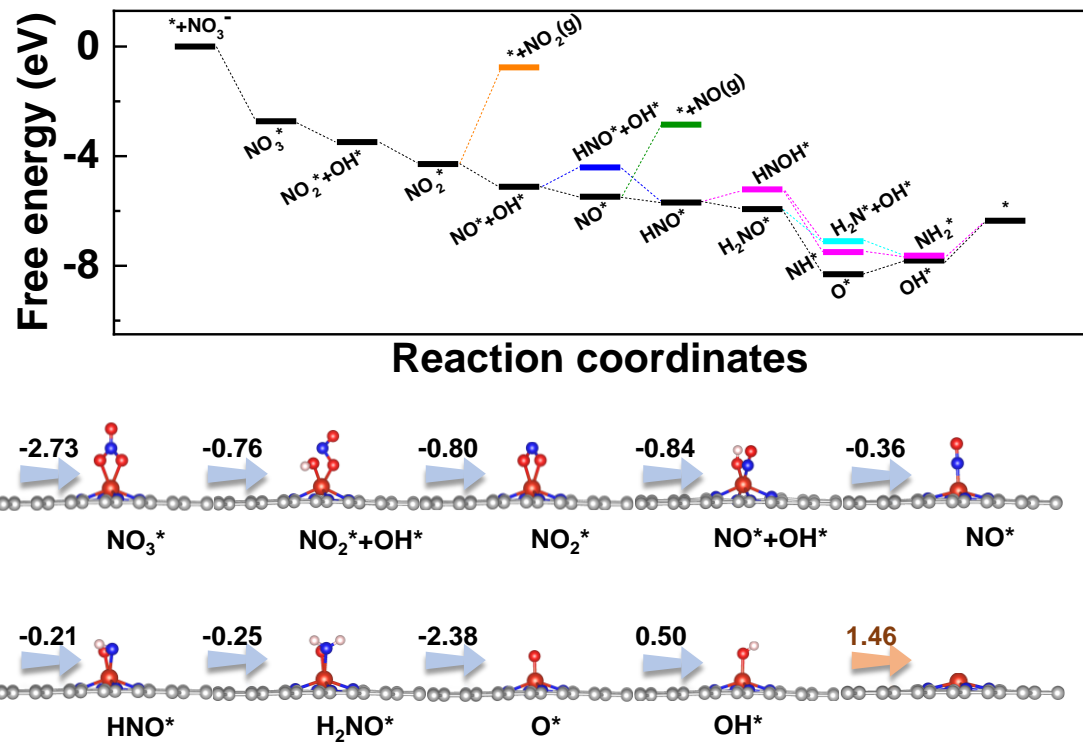


Fig. S12. Free energy diagram together with the configurations of corresponding intermediates for the eNO₃RR on VN₄@G.

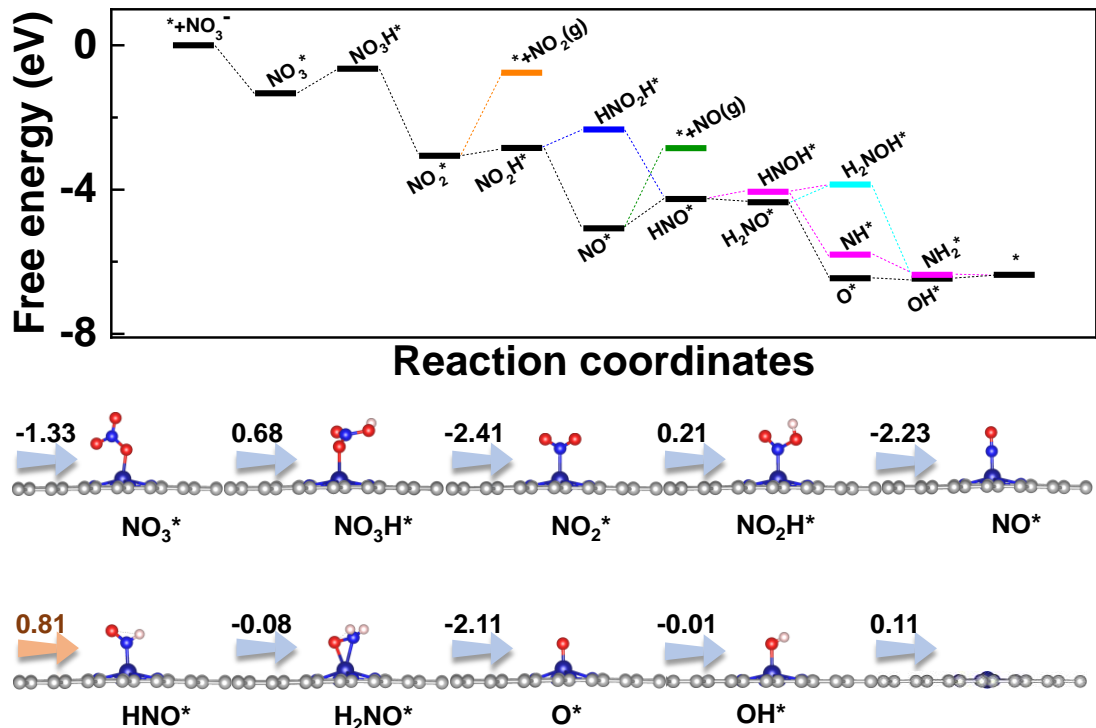


Fig. S13. Free energy diagram together with the configurations of corresponding intermediates for the eNO₃RR on CrN₄@G.

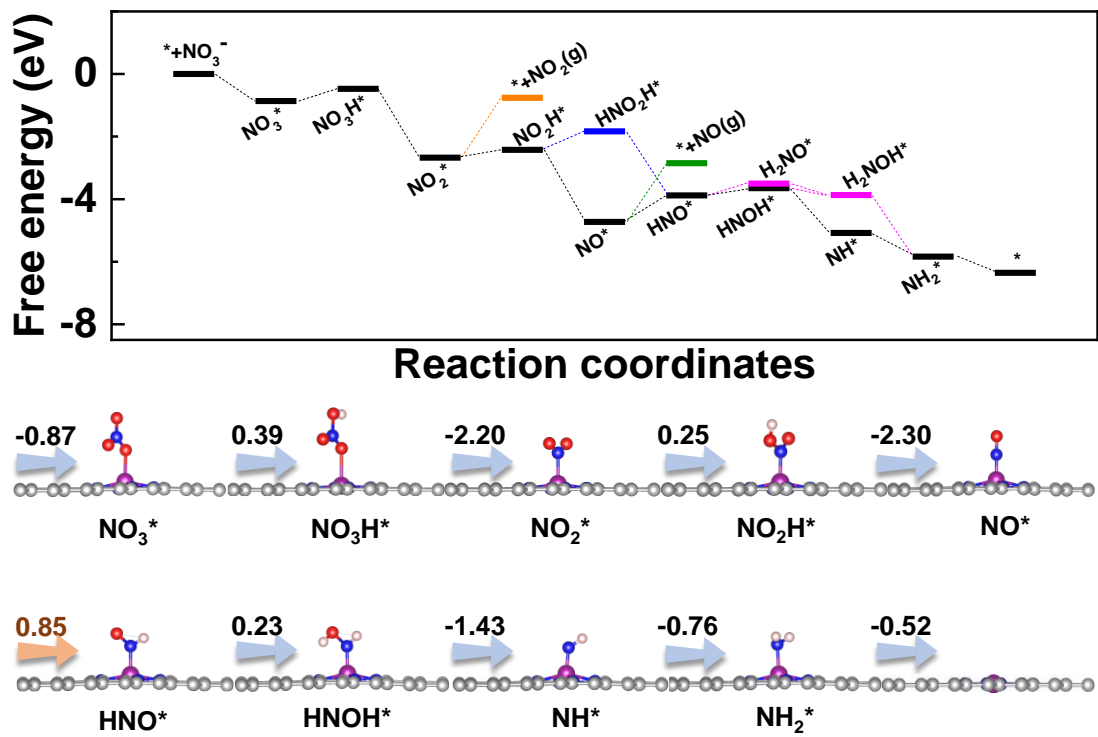


Fig. S14. Free energy diagram together with the configurations of corresponding intermediates for the eNO₃RR on MnN₄@G.

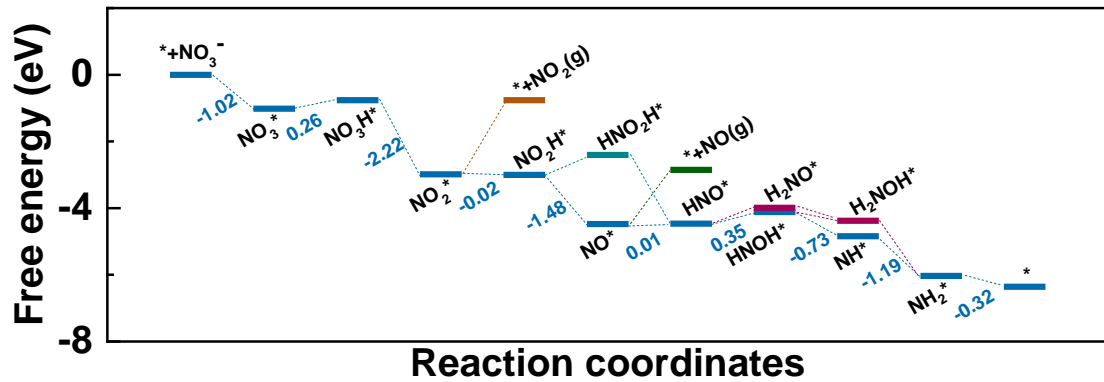


Fig. S15. Free energy diagram for the eNO₃RR on FeN₄@G with consideration of the solvation effect.

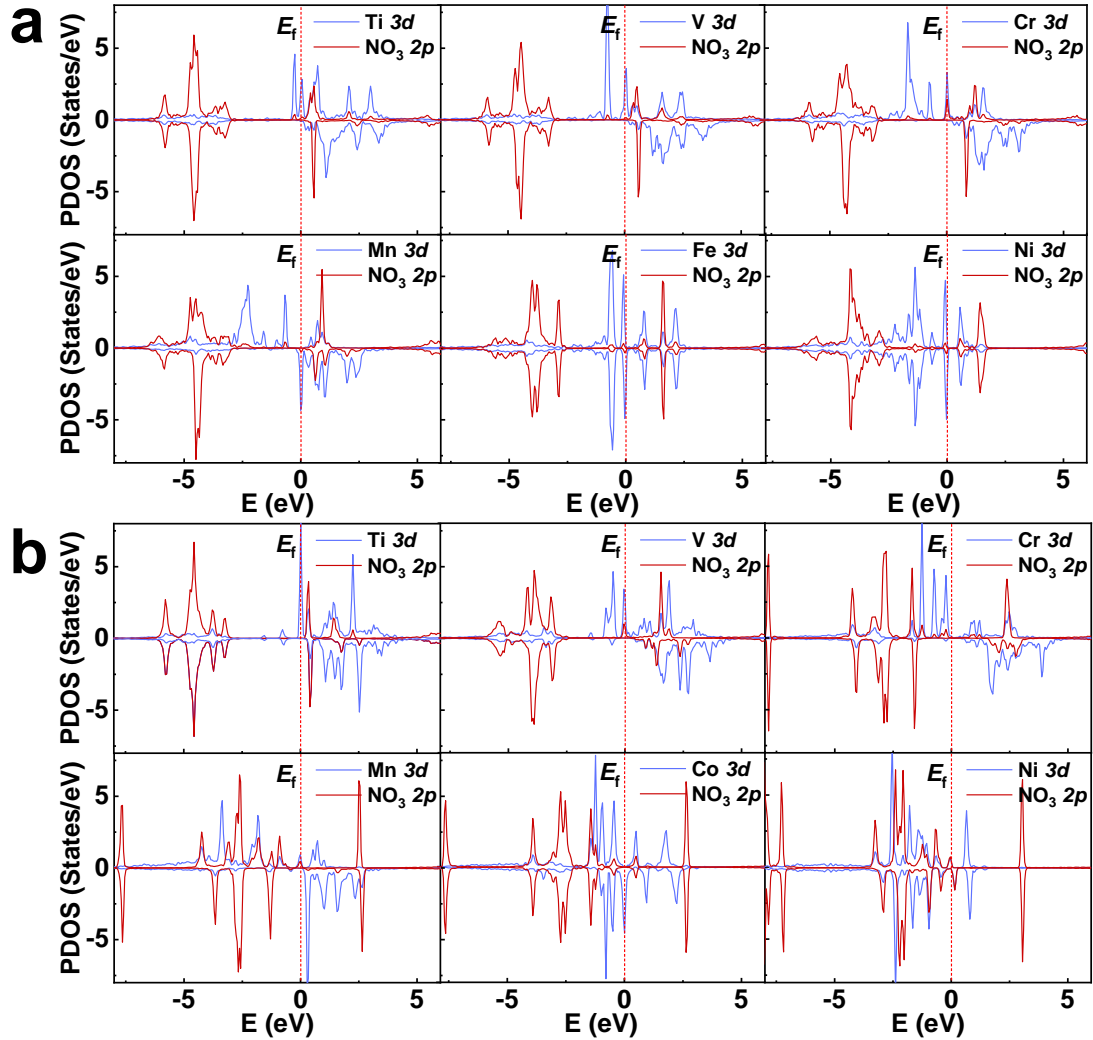


Fig. S16. Projected densities of states (PDOS) of the TM 3d states and O (in NO_3^*) 2p states, which is bonded with the TM atom. (a) and (b) are for $\text{TMN}_3@\text{G}$ and $\text{TMN}_4@\text{G}$, respectively. The vertical dashed line denotes the position of Fermi level (E_f). The positive and negative values of TDOS correspond to the spin-up and spin-down states, respectively.

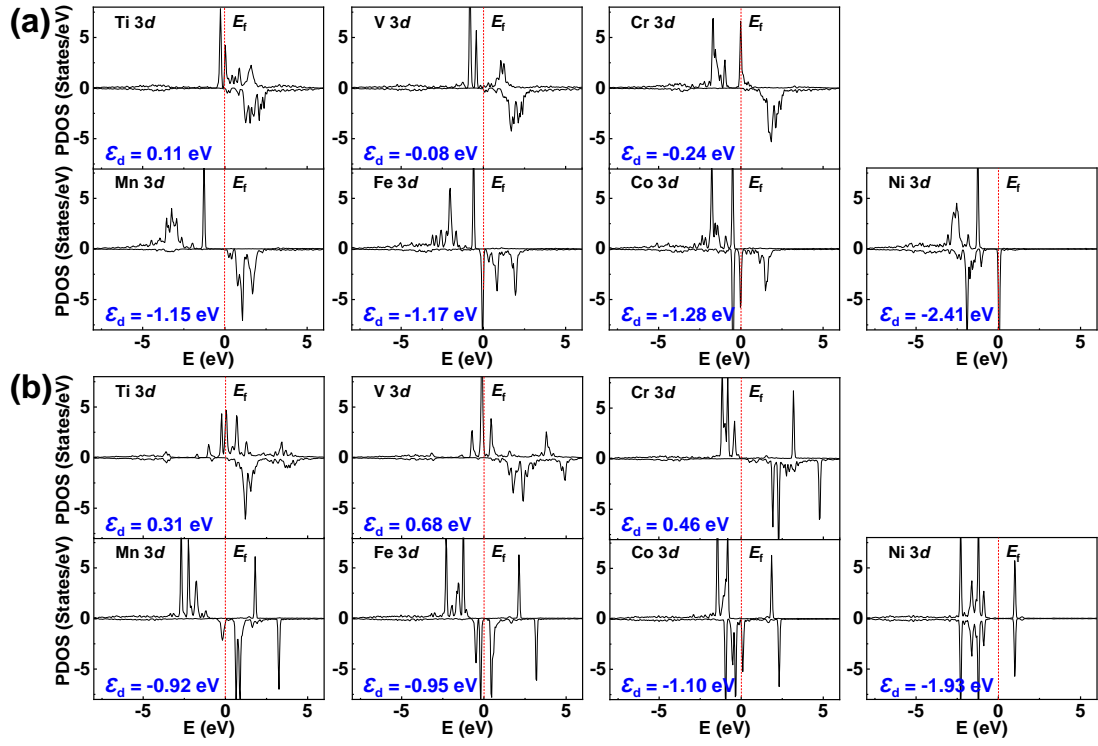


Fig. S17. Projected densities of state (PDOS) and the d-band center (ε_d) of the TM 3d states of the pristine $\text{TMN}_3@\text{G}$ and $\text{TMN}_4@\text{G}$. The vertical dashed line denotes the position of Fermi level (E_f). The positive and negative values of TDOS correspond to the spin-up and spin-down states, respectively.

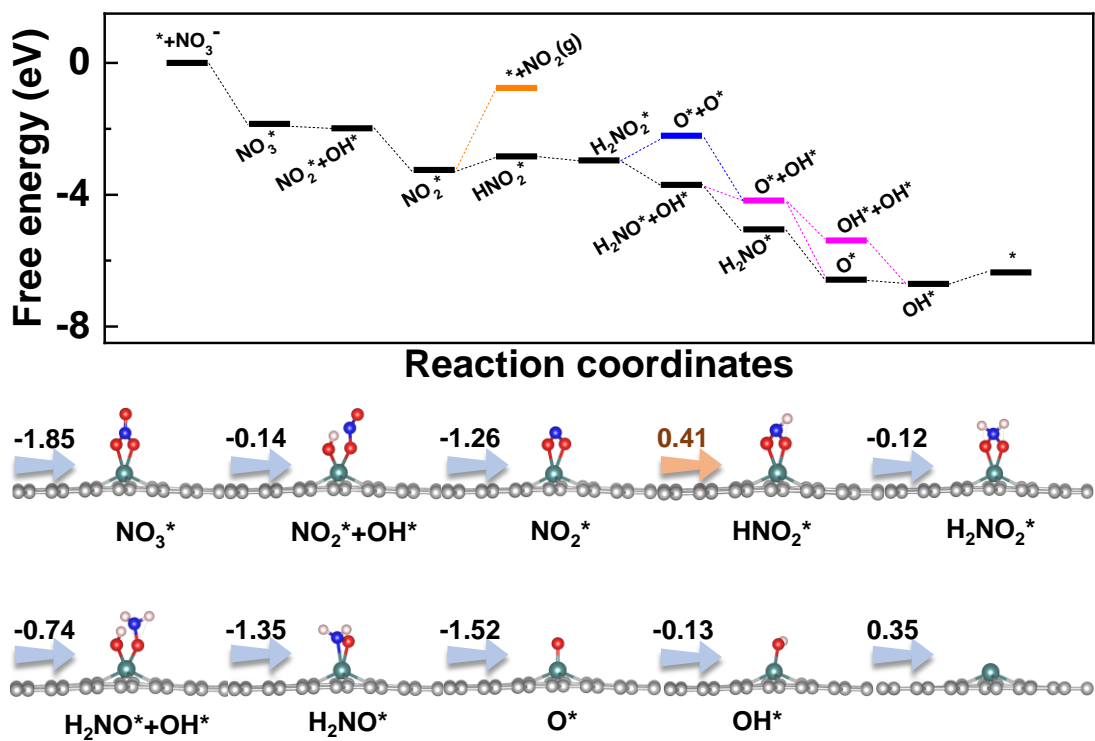


Fig. S18. Free energy diagram together with the configurations of corresponding intermediates for the e NO_3 RR on $\text{RuC}_4@\text{G}$.

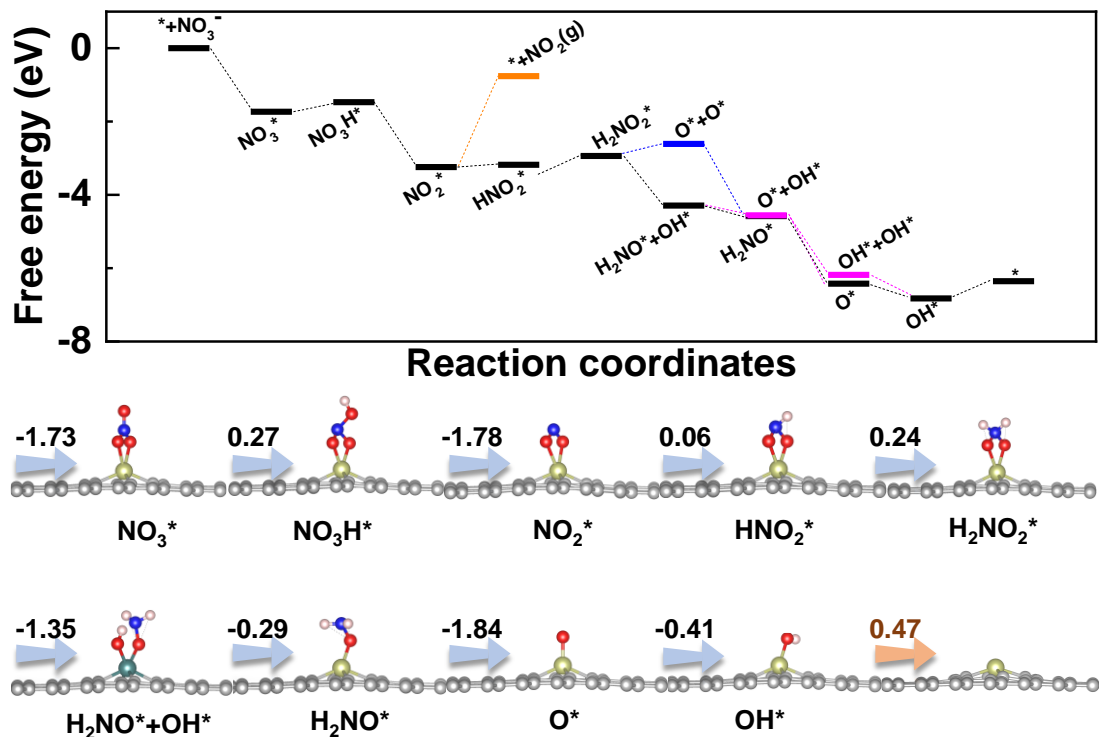


Fig. S19. Free energy diagram together with the configurations of corresponding intermediates for the e NO_3 RR on $\text{IrC}_4@\text{G}$.